MITSUBISHI HEAVY INDUSTRIES, LTD.
16-5, KONAN 2-CHOME, MINATO-KU
TOKYO, JAPAN

November 6, 2009

Document Control Desk
U.S. Nuclear Regulatory Commission
Washington, DC 20555-0001

Attention: Mr. Jeffrey A. Ciocco

Docket No. 52-021
MHI Ref: UAP-HF-09512

Subject: **MHI's 2nd Response to the NRC's Request for Additional Information on Topical Report MUAP-07013-P (R0) "Small Break LOCA Methodology for US-APWR" on 09/08/2009**

Reference: 1) "REQUEST FOR ADDITIONAL INFORMATION ON TOPICAL REPORT MUAP-07013-P, ' SMALL BREAK LOCA METHODOLOGY FOR US-APWR'," dated on September 8, 2009.

With this letter, Mitsubishi Heavy Industries, Ltd. ("MHI") transmits to the U.S. Nuclear Regulatory Commission ("NRC") an official document entitled 'MHI's 2nd Response to the NRC's Request for Additional Information on Topical Report MUAP-07013-P (R0) "Small Break LOCA Methodology for US-APWR" on 09/08/2009'. In the enclosed document, MHI provides the 14 (fourteen) out of 40 (forty) items requested in Reference 1. The remaining responses to the RAI in Reference 1 were transmitted to the NRC by separate correspondence on October 23, 2009 (45 days after the issuance of the formal RAI), as agreed by NRC and MHI.

As indicated in the enclosed materials, this document contains information that MHI considers proprietary, and therefore should be withheld from public disclosure pursuant to 10 C.F.R. § 2.390 (a)(4) as trade secrets and commercial or financial information which is privileged or confidential. A non-proprietary version of the document is also being submitted in this package (Enclosure 3). Any proprietary information that is written inside a bracket in the proprietary-version is replaced by the designation "[ ]" without any text, in the non-proprietary-version.

This letter includes a copy of proprietary version (Enclosure 2), a copy of non-proprietary version (Enclosure 3), and the Affidavit of Yoshiki Ogata (Enclosure 1) which identifies the bases of MHI request that all materials designated as "Proprietary" in Enclosure 2 be withheld from public disclosure pursuant to 10 C.F.R. § 2.390 (a)(4).

Please contact Dr. C. Keith Paulson, Senior Technical Manager, Mitsubishi Nuclear Energy Systems, Inc. if the NRC has questions concerning any aspect of this submittal. His contact information is provided below.

Sincerely,

Y. Ogata

Yoshiki Ogata
General Manager - APWR Promoting Department
Mitsubishi Heavy Industries, LTD.

D081
NRO

Enclosures:

1. Affidavit of Yoshiki Ogata

2. MHI's 2nd Response to the NRC's Request for Additional Information on Topical Report MUAP-07013-P (R0) "Small Break LOCA Methodology for US-APWR" on 09/08/2009 (proprietary)

3. MHI's 2nd Response to the NRC's Request for Additional Information on Topical Report MUAP-07013-P (R0) "Small Break LOCA Methodology for US-APWR" on 09/08/2009 (non-proprietary)

CC: J. A. Ciocco
C. K. Paulson

Contact Information
C. Keith Paulson, Senior Technical Manager
Mitsubishi Nuclear Energy Systems, Inc.
300 Oxford Drive, Suite 301
Monroeville, PA 15146
E-mail: ck_paulson@mnes-us.com
Telephone: (412) 373 – 6466

ENCLOSURE 1

Docket No.52-021
MHI Ref: UAP-HF-09512

MITSUBISHI HEAVY INDUSTRIES, LTD.

AFFIDAVIT

I, Yoshiki Ogata, being duly sworn according to law, depose and state as follows:

1. I am General Manager, APWR Promoting Department, of Mitsubishi Heavy Industries, Ltd ("MHI"), and have been delegated the function of reviewing MHI's US-APWR documentation to determine whether it contains information that should be withheld from disclosure pursuant to 10 C.F.R. § 2.390 (a)(4) as trade secrets and commercial or financial information which is privileged or confidential.

2. In accordance with my responsibilities, I have reviewed the enclosed "MHI's 2nd Response to the NRC's Request for Additional Information on Topical Report MUAP-07013-P (R0) 'Small Break LOCA Methodology for US-APWR' on 09/08/2009" and have determined that portions of the report contain proprietary information that should be withheld from public disclosure. Those pages containing proprietary information are identified with the label "Proprietary" on the top of the page and the proprietary information has been bracketed with an open and closed bracket as shown here "[ ]". The first page of the technical report indicates that all information identified as "Proprietary" should be withheld from public disclosure pursuant to 10 C.F.R. § 2.390 (a)(4).

3. The information in the report identified as proprietary by MHI has in the past been, and will continue to be, held in confidence by MHI and its disclosure outside the company is limited to regulatory bodies, customers and potential customers, and their agents, suppliers, and licensees, and others with a legitimate need for the information, and is always subject to suitable measures to protect it from unauthorized use or disclosure.

4. The basis for holding the referenced information confidential is that it describes the unique codes and files developed by MHI for the fuel of the US-APWR and also contains information provided to MHI under license from the Japanese Government. These codes and files were developed at significant cost to MHI, since they required the performance of detailed calculations, analyses, and testing extending over several years. The referenced information is not available in public sources and could not be gathered readily from other publicly available information. MHI knows of no way the information could be lawfully acquired by organizations or individuals outside of MHI and the Japanese Government.

5. The referenced information is being furnished to the Nuclear Regulatory Commission ("NRC") in confidence and solely for the purpose of supporting the NRC staff's review of MHI's Application for certification of its US-APWR Standard Plant Design.

6. Public disclosure of the referenced information would assist competitors of MHI in their design of new nuclear power plants without the costs or risks associated with the design of new fuel systems and components. Disclosure of the information identified as proprietary would therefore have negative impacts on the competitive position of MHI in

the U.S. nuclear plant market.

I declare under penalty of perjury that the foregoing affidavit and the matters stated therein are true and correct to the best of my knowledge, information and belief.

Executed on this 6th day of November, 2009.

Y. Ogata

Yoshiki Ogata
General Manager- APWR Promoting Department
Mitsubishi Heavy Industries, LTD.

ENCLOSURE 3

UAP-HF-09512

MHI's 2nd Response to the NRC's Request for Additional Information on Topical Report MUAP-07013-P (R0) "Small Break LOCA Methodology for US-APWR" on 09/08/2009

November 2009
(Non-Proprietary)

REQUEST 3-2

[

]

RESPONSE

[

]

[

]

REQUEST 8.1.4-11

[

]

RESPONSE

[

]

REQUEST 8.2.1-8

[

]

RESPONSE

[

]

REQUEST 8.2.1-9

[

]

RESPONSE

[

]

REQUEST 8.2.1-10

On page 8.2.1-7 MHI defines the time period from 50 s to 95 s as the natural circulation period. According to the pump coastdown curves (Figure 8.2.1-11 and 8.2.1-12), however, the pump speed is still high during that period (about 5/8 of the initial speed at 50 s and about 5/16 of the initial speed at 95 s). So the flow rate seems to be still primarily determined by the pumps. Please justify quantitatively that the time period of 50 s to 95 s can be defined as the natural circulation period.

RESPONSE

As described previously in the response to REQUEST 4-1 (Ref. 1), the natural circulation period starts (the blowdown period ends) when the primary system pressure has decreased to nearly that of the secondary system. The natural circulation period ends when the liquid flow rate at the top of SG U-tubes decreases to zero. During this period, the RCP pump head is expected to be zero or negative, since the RCP trips concurrently with the reactor trip in the accident scenario for the US-APWR LOCAs.

Figure RAI-8.2.1-10.1 shows temporal changes of the primary and secondary pressures. The period from 50 to 95 seconds is identified as the natural circulation phase based on the definition described above. During this period, the RCP head stayed below zero, as shown in Figures RAI-8.2.1-10.2 and 3, which indicates that the primary mass flowrate was not determined by the pumps, but instead was determined by natural circulation.

Reference:

1. Mitsubishi Heavy Industries, Ltd., MHI's Partial Responses to the NRC's Requests for Additional Information on Topical Report MUAP-07013-P (R0) "Small Break LOCA Methodology for US-APWR", UAP-HF-09002-P (R0), January 16, 2009.

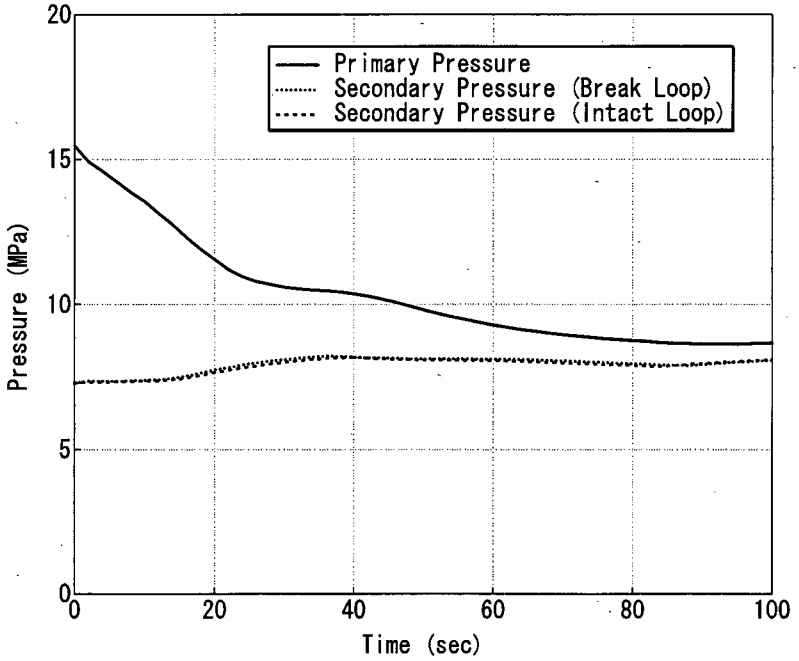

Figure 8.2.1-10.1 Primary and Secondary Pressures

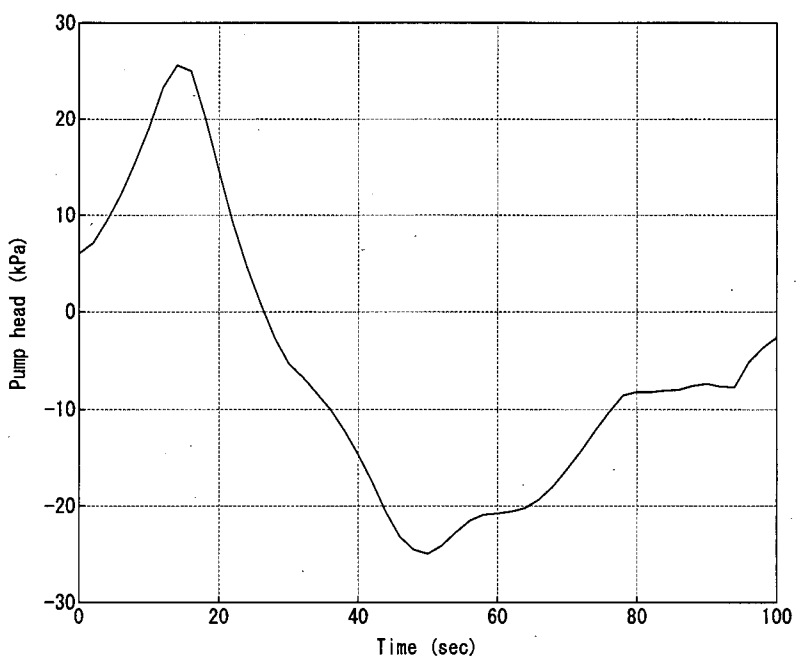

Figure 8.2.1-10.2 Pump Head (Broken Loop)

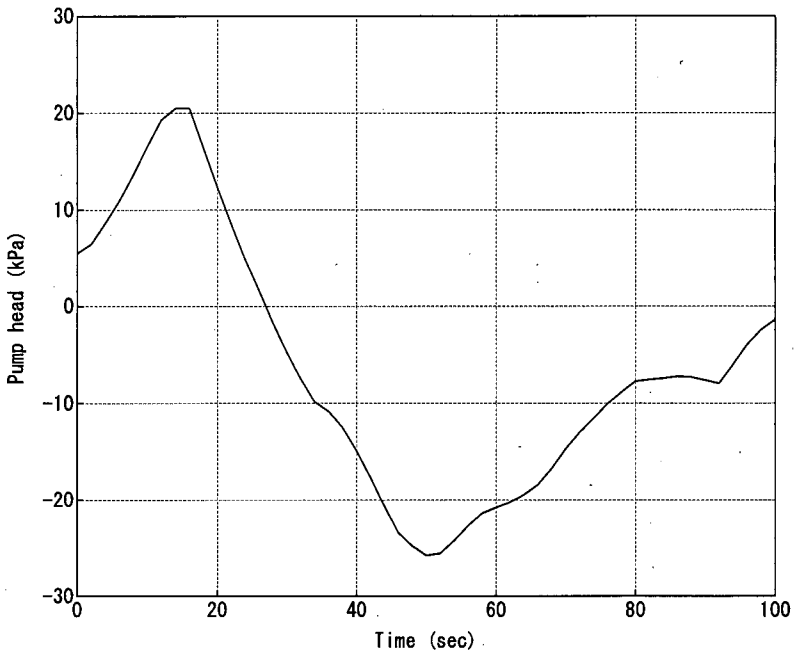

Figure 8.2.1-10.3 Pump Head (Intact Loop)

REQUEST 8.2.1-11

On page 8.2.1-7 MHI states, "Both loops flowrate at cross-over leg of M-RELAP5 calculation agree with these of the test data during natural circulation period (Figure 8.2.1-18 and 19). As a result, M-RELAP5 capability to predict SG primary and secondary heat transfer is good."

As discussed in RAI 8.2.1-10, the loop flowrate seems to be mostly determined by the pump speed during that time period. And the pump coastdown curve was given as an input. As a result, it is obvious that the predicted loop flowrate agrees well with the test data. MHI's conclusion above regarding the heat transfer prediction being good is based on an essentially specified flow rate, a major determinant of the heat transfer coefficients. Please explain how this assessment is useful for assessing M-RELAP5 for application to the US-APWR SBLOCA where the flow rate must be predicted by the code.

RESPONSE

The response to REQUEST 8.2.1-10 showed that the primary coolant flowed under the natural circulation condition. The primary flowrate was primarily dependent on the coolant vaporization in the core and steam condensation in the SG during the identified time period (50-95 seconds). Heat removal to the secondary system is modeled to simulate the steam condensation in the present code assessment. The capability of M-RELAP5 to predict the heat transfer in the SG is discussed in the response to REQUEST 8.2.1-12.

REQUEST 8.2.1-12

The 2nd last paragraph on page 8.2.1-7 states, "Break flowrate of M-RELAP5 calculation is adjusted to test data (Figure 8.2.1-15), as a result, primary pressure drop behavior agrees with test data excellently (Figure 8.2.1-16). Signal timings agree with test data (Table 8.2.1-6). Secondary pressures are also adjusted to test data (Figure 8.2.1-13 and 8.2.1-14). Primary pressure and secondary pressures of M-RELAP5 calculation agree with test data, as a result, M-RELAP5 capability to predict SG primary and secondary heat transfer is good."

It is obvious that the primary and secondary system pressures show good agreements between the prediction and the measurement because the primary system pressure was predicted with the adjusted break flow and the secondary system pressure was also adjusted to the test data. Since this is not the manner in which the plant calculations will be performed, i.e. break flow and secondary pressure will not be specified as boundary conditions, please explain how this assessment establishes the ability of M-RELAP5 to predict the plant response for SBLOCA events.

RESPONSE

Followings are the quantitative evaluation result that MHI stated in the previous response to this REQUEST (Ref. 1).

MHI has performed an additional sensitivity analysis where mechanical motions of the main steam isolation and relief valves are modeled with the VALVE components. SG secondary pressure transients are shown in Figures RAI-8.2.1-12.1 and 2. The heat transfer through the SG U-tubes is validated by comparing the integral of steam mass discharged out the main steam isolation and relief valves between the calculation and measurement. It is noted that SG primary and secondary side heat transfers are identified as high-ranked phenomena during the blowdown, natural circulation, and loop seal clearance phases in the US-APWR SBLOCA PIRT (Ref. 2).

Although M-RELAP5 overestimates the steam released from the SGs as shown in Figures RAI-8.2.1-12.3, the difference between the calculation and measurement of the total discharge is less than 10%. This overestimation is negligibly small from the impact to the primary system pressure response as confirmed in Figure RAI-8.2.1-12.4. In addition, Figure RAI-8.2.1-12.5 shows that the core liquid level (differential pressure) in the sensitivity calculation agrees with that obtained by the base model described in the topical report (Ref. 1). This fact suggests that the code assessment results presented in the topical report are sufficiently meaningful, even though the secondary system pressure is imposed by the boundary condition there.

References:

1. Mitsubishi Heavy Industries, Ltd., MHI's 1st Response to the NRC's Request for Additional Information on Topical Report MUAP-07013-P (R0) "Small Break LOCA Methodology for US-APWR" on 09/08/2009, UAP-HF-09492-P (R0), October 23, 2009.
2. Mitsubishi Heavy Industries, Ltd., Small Break LOCA Methodology for US-APWR, MUAP-07013-P (R0), July 2007.

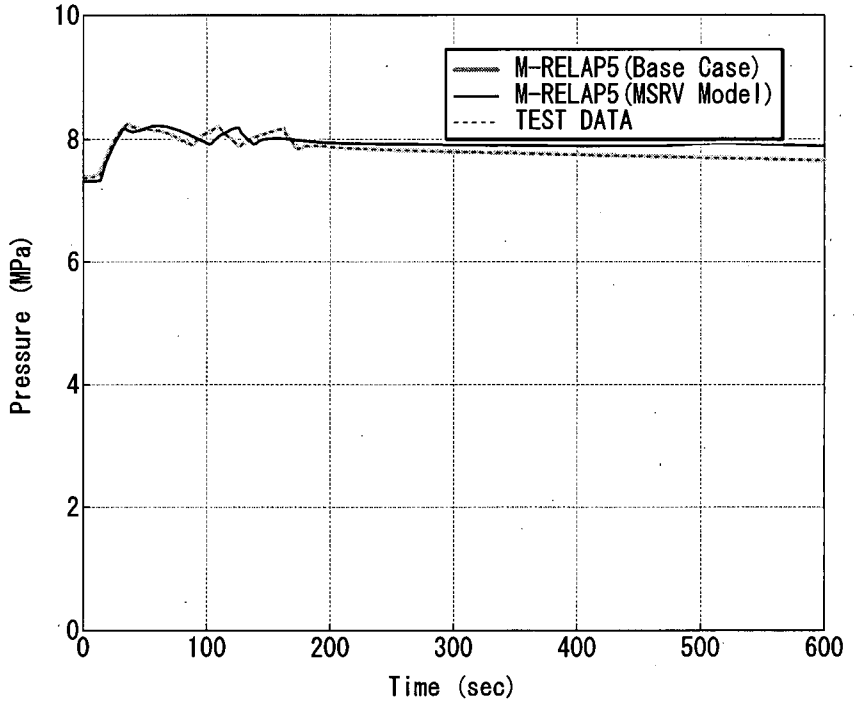

Figure 8.2.1-12.1 Broken Loop Secondary Pressure

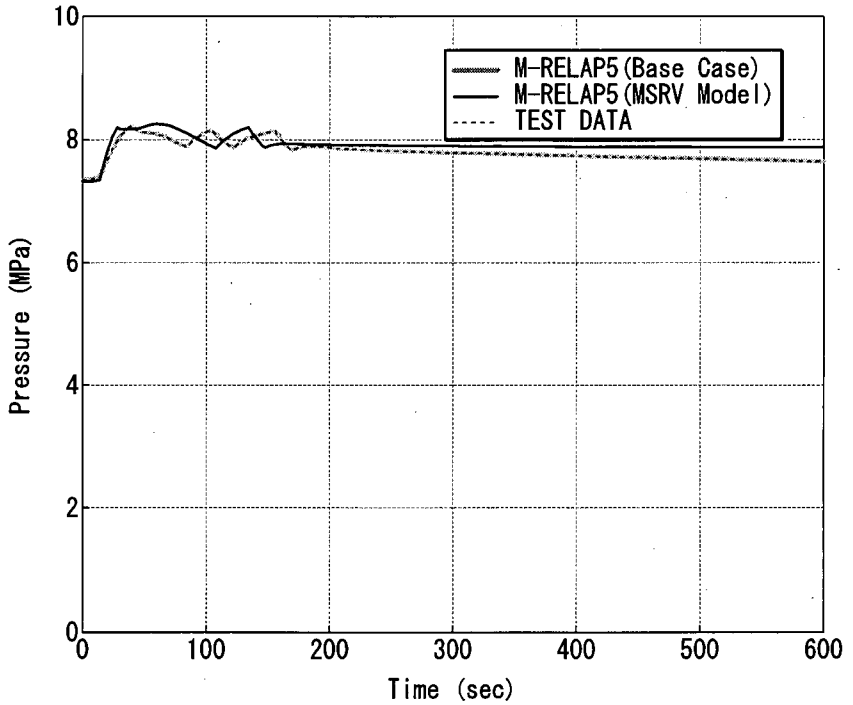

Figure 8.2.1-12.2 Intact Loop Secondary Pressure

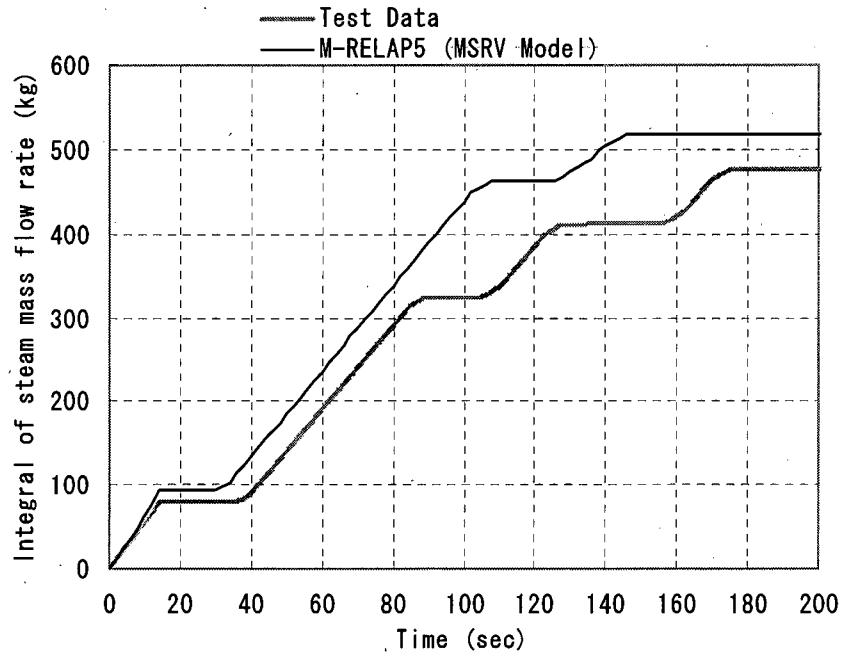

Figure 8.2.1-12.3 Integral of SG Secondary Outlet Steam Mass

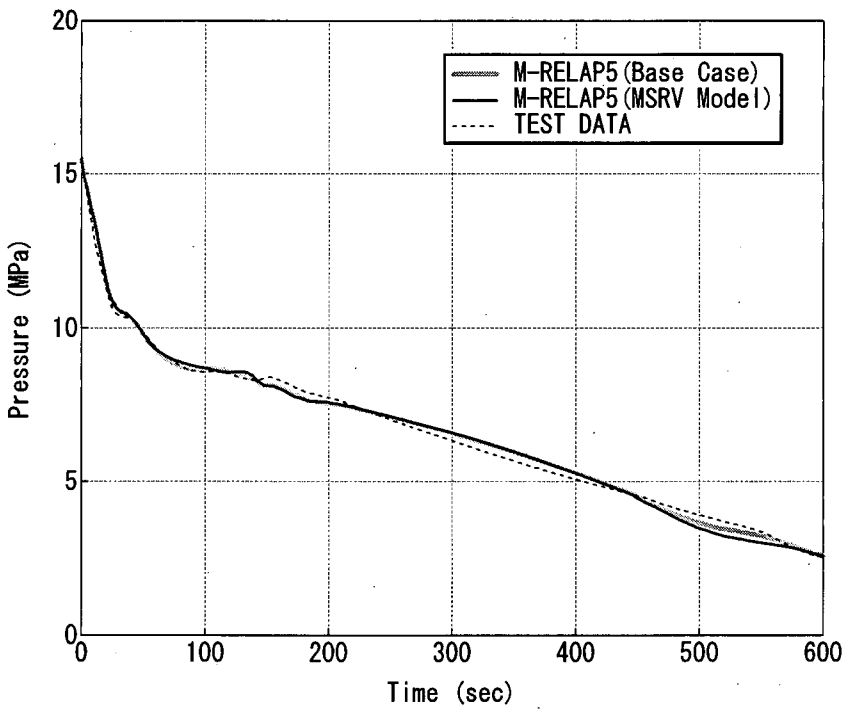

Figure 8.2.1-12.4 Pressurizer pressure

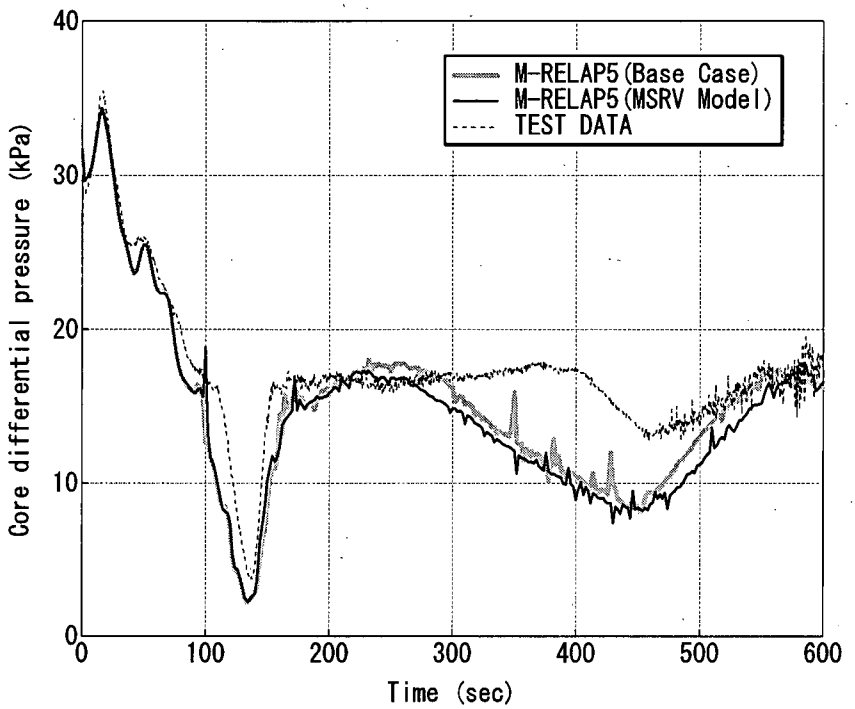

Figure 8.2.1-12.5 Core Differential Pressure

REQUEST 8.2.1-13

The 2nd paragraph on page 8.2.1-8 states, "Downcomer water level of M-RELAP5 result agrees with that of test data at about 150 sec (Figure 8.2.1-34). As a result, M-RELAP5 capability to predict downcomer mixture level is good during loop seal period."

Figure 8.2.1-34 shows that the predicted behavior of the downcomer water level (in terms of differential pressure) is different from the measured data until around 150 s. Explain this difference.

The initial differential pressure is higher in the simulation than in the experiment by around 3 kPa. Does this mean that the measurement points of the differential pressure are different between the simulation and the test? Explain why there is approximately a 3 kPa difference in the differential pressure at time zero.

RESPONSE

The M-RELAP5 noding diagram for the ROSA-IV/LSTF calculation and the axial locations for the downcomer differential pressure measurement are shown in Figure RAI-8.2.1-13.1. The predicted differential pressure between Location 1 and Location 2 was used in the Figure 8.2.1-34 of MUAP-07013-P (Ref. 1). Location 1 is the center of component 100, and Location 2 is the middle of the centers of components 112 and 116. These axial locations are different from those for the measurement as shown in Figure RAI-8.2.1-13.1. The differential pressure for the measurement locations is obtained from the calculation results and is compared with the measurement data in Figure RAI-8.2.1-13.2. The calculated initial differential pressure agrees with the measurement data.

The initial coolant temperature in the upper downcomer above the cold leg [ ] is not adequately calculated in the steady state initialization because the coolant temperature of [ ] is not accurately calculated by the one-dimensional nodalization and then the heat transfer from [ ] through the wall is not accurately calculated. As the initial core power of the ROSA-IV/LSTF is 14% of the scaled power, the initial loop flow rate is also reduced to 14% of the scaled flow rate (Ref. 2). And the bypass flow between the downcomer and the upper head is 0.3% of the rated core flow [ ]. As the flow rate into the upper downcomer is small, the coolant stays there for a long time. The heat transferred from the coolant having the hot leg temperature that occurred in the upper plenum and the upper head through the wall cannot be neglected. It is estimated that the initial coolant temperature in the upper downcomer is higher than the cold leg temperature and is near the primary coolant system average temperature. The obtained temperature in the original steady state initialization is slightly higher than the cold leg temperature.

The sensitivity calculation was performed to investigate the effect of the initial coolant temperature in the upper downcomer on the differential pressure of the downcomer. In this calculation, the initial coolant temperature in the upper downcomer region is set to the primary coolant average temperature, and also the temperatures in thermal equilibrium with the adjacent coolant are applied for the heat structures in the upper downcomer and also the upper head. In the original calculation, the measured temperature near the hot leg temperature is already applied to the coolant in the upper head, but the cold leg

temperature is still applied to the heat structures in the upper head. [

]

The calculated result is shown in Figure RAI-8.2.1-13.3. The predicted differential pressure decreases more before 150 seconds and agrees better with the measurement than the original calculation. As the initial coolant temperature in the upper downcomer is higher and the coolant warmed by the heat transfer from the heat structure in the upper head comes through the spray nozzle in the present calculation, the coolant in the upper downcomer begins to flash earlier as the primary coolant system depressurizes and this flashing pushes out hotter coolant to the lower downcomer. The flashing in the upper downcomer and the coolant temperature increase in the lower downcomer decrease the differential pressure in the downcomer. The predicted core differential pressure is shown in Figure RAI-8.2.1-13.4 compared with the original calculation. The changes of the initial coolant temperature in the upper downcomer, the initial heat structure temperature in the upper part of the reactor vessel [ ] hardly affect the other parameters rather than the differential pressure in the downcomer.

The over-prediction of the differential pressure of the downcomer until around 150 seconds in MUAP-07013-P is considered to be caused by the initial coolant temperature in the upper downcomer, the initial heat structure temperature in the upper part of the reactor vessel [ ].

References:

1. Mitsubishi Heavy Industries, Ltd., Small Break LOCA Methodology for US-APWR, MUAP-07013-P (R0), July 2007.
2. "ROSA-IV/LSTF 5% Clod Leg Break LOCA Experiment Run SB-CL-18 Data Report," JAERI-M89-027, March 1989.

Figure RAI-8.2.1-13.1 The M-RELAP5 Noding Diagram and Differential Pressure Measurement Location

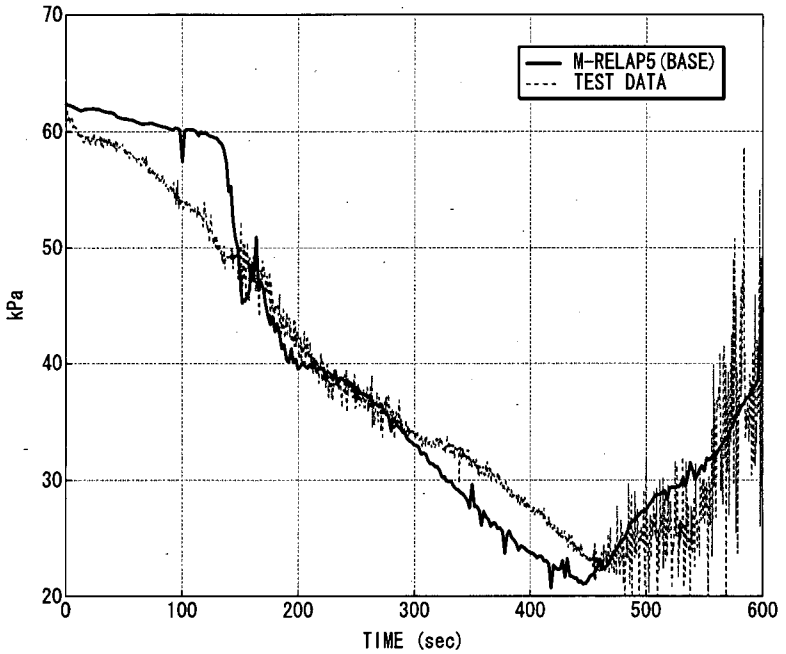

Figure RAI-8.2.1-13.2 Downcomer Differential Pressure (Locations are adjusted)

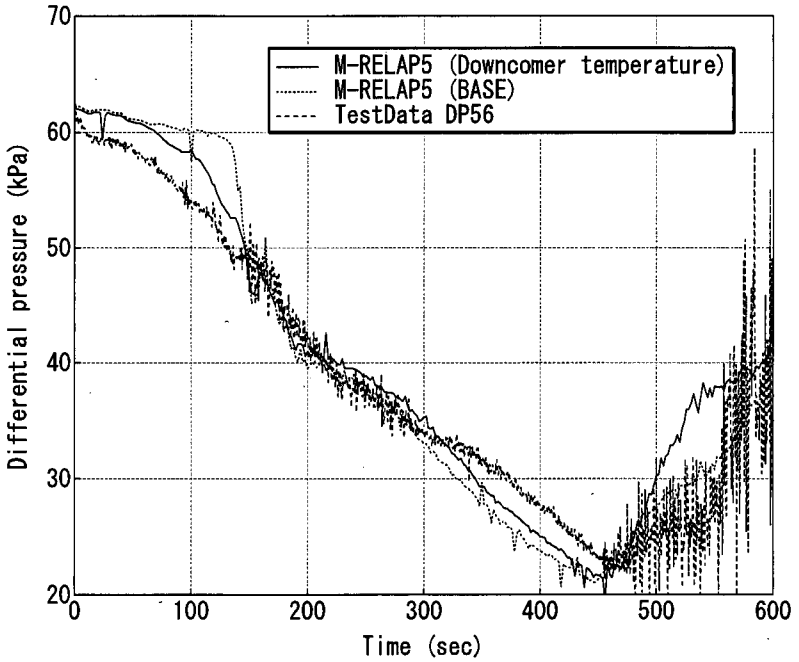

Figure RAI-8.2.1-13.3 Downcomer Differential Pressure (Revised Models are applied)

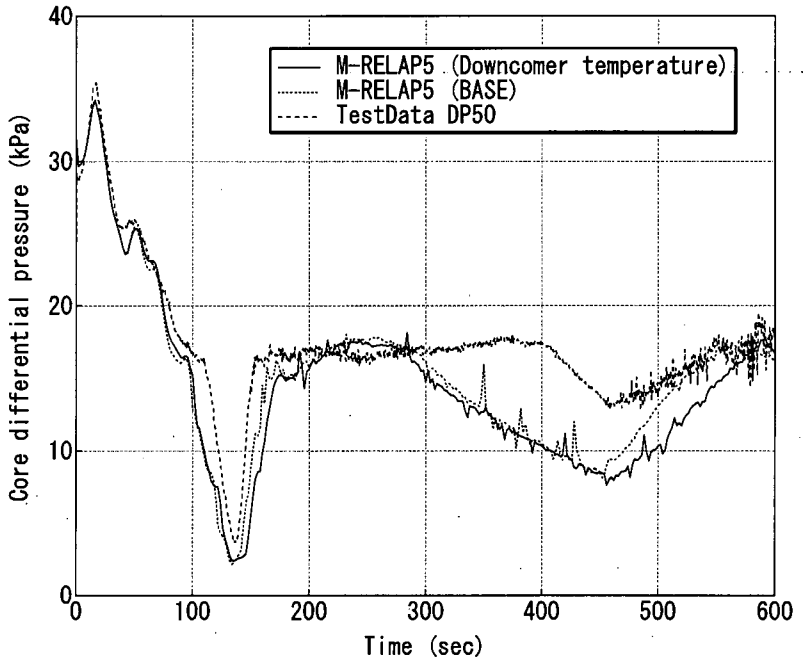

Figure RAI-8.2.1-13.4 Core Differential Pressure

REQUEST 8.2.1-16
(Related RAI 8.2.1-6)
[

]

RESPONSE
[

]

REQUEST 8.2.1-18

Figures 8.2.1-39 and 8.2.1-40 show that M-RELAP5 predicts the heater rod rewetting occurred slightly earlier at 3.57 m at around 550 s than at 3.17 m at around 560 s while the heater rod is rewetted first at 3.17 m at around 500 s and then at 3.57 m at around 540 s in the test. Explain why the heater rod rewetting occurs later at the lower section (at 3.17 m) than the upper section (at 3.57 m) in the simulation whereas the test data shows that the rewetting occurs later at the upper section.

RESPONSE

The rewetting phenomenon during the core recovery phase is discussed here. During the core recovery and the preceding boil-off phases, the core is covered almost by single-phase vapor in the region above the mixture level. The predicted heater rod temperature transients at various elevations are shown in Figure RAI-8.2.1-18.1. The heater rod heat-up occurs systematically from the upper elevation to the lower elevation during the boil-off phase as the core mixture level decreases. Also, the heater rod rewetting occurs systematically from the lower elevation to the upper elevation during the core recovery phase as the core mixture level increases until the rewetting elevation reaches 3.17m. However, the heater rod rewetting occurs earlier at the upper elevation of 3.57m compared to that at 3.17m.

[

] The void fractions at the elevation of 3.17m and 3.57m are shown in Figure RAI-8.2.1-18.2. The upper elevation of 3.57m has a larger void fraction and poorer heat transfer to the fluid near the rewetting time. As the axial rod power distribution used in the ROSA-IV/LSTF experiments is cosine, the power generation rate at the upper section is small and the heater rod temperature rise during the core uncovery is also small as shown in Figure RAI-8.2.1-18.1. It is considered that the heater rod temperature is dominant for the rewetting phenomena compared to the fluid condition at the upper section and the upper section rewets earlier. Even so, the rewetting at 3.57m elevation is conservatively predicted compared to the experimental data as shown Figure 8.2.1-39 of MUAP-07013-P (Ref. 1).

Reference

1. Mitsubishi Heavy Industries, Ltd., Small Break LOCA Methodology for US-APWR, MUAP-07013-P (R0), July 2007.

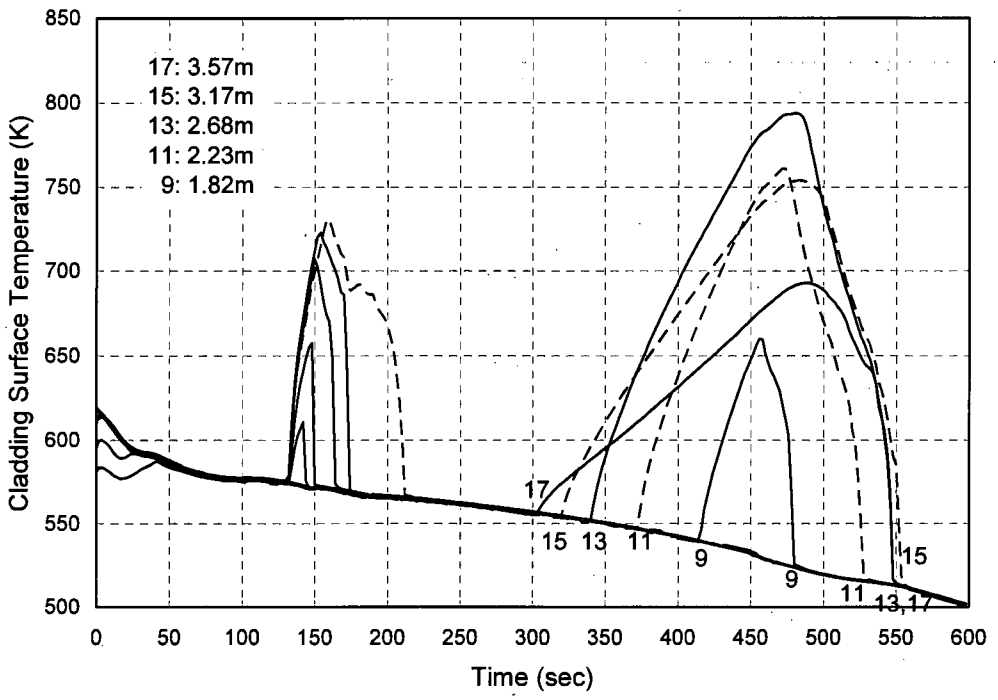

Figure RAI-8.2.1-18.1 Heater Rod Surface Temperature

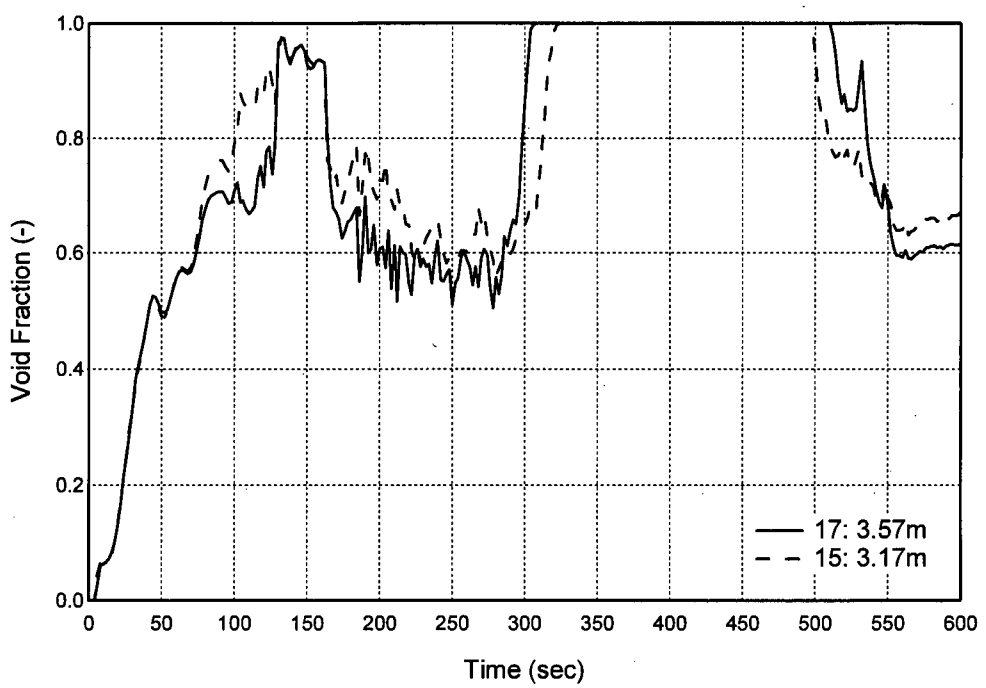

Figure RAI-8.2.1-18.2 Void Fraction at Upper Elevations

REQUEST 8.2.1-19

The 2nd paragraph on page 8.2.1-11 says, "There are some heater rods heated up at such a upper portion in the experimental data. It indicates that the accumulated water on the upper plenum region partly flow down to the core region. This is consistent with the view that a spatially non-uniform liquid distribution exists in the core region. Such liquid distribution effects are already modeled as CHF multiplier in M-RELAP5. But this base case results indicate that this CHF multiplier is not enough for ROSA-IV/LSTF SBLOCA analysis."

The meaning of the above quotation is not clear. Explain how the flowing down of the accumulated water from the upper plenum region is related to the heater rods heating up in the upper portion of the core region in the experimental data. Explain how the liquid distribution effects are modeled in M-RELAP5 with the CHF multiplier. Describe the specific multiplier that is referred to and why it is not enough for ROSA-IV/LSTF SBLOCA analysis.

RESPONSE

The vapor generated by the core decay heat flows into the steam generator and condenses there during the loop seal clearance phase. The liquid-condensate due to the condensation heat transfer in the uphill side of steam generator flows back into the upper plenum via hot leg and the accumulated liquid in the upper plenum drains into the core. The drained liquid flows down on the fuel rod surface as the liquid film. CHF occurs when the liquid film on the fuel rod surface disappears. The liquid flow rate into the core is expected to non-uniformly distribute in the radial and azimuthal directions by complex multi-dimensional two-phase flow phenomena. Then, CHF initially occurs at less rod surface heat flux compared with the situation in which the liquid flows down uniformly into the core.

The rod surface temperatures were measured in many heater rods which are radially and azimuthally distributed and at several axial locations in the ROSA-IV/LSTF SB-CL-18 experiment. The heater rod surface temperatures in the high power region in the upper core during the loop seal clearance period are shown in Figure RAI-8.2.1-19.1 and Figure RAI-8.2.1-19.2. The locations of these heater rods are shown in Figure RAI-8.2.1-19.3. Most heater rods experience CHF, but several heater rods do not experience CHF at both elevation. The CHF occurrence time varies for each rod and is not closely correlated with elevations. The rod surface temperature transients during the boil-off and core recovery phases of the same heater rods are shown in Figure RAI-8.2.1-19.4 and Figure RAI-8.2.1-19.5. As the liquid does not flow down into the core from the upper plenum during these periods, all heater rods experience CHF and the CHF proceeds from the lower elevations to the higher ones. So, the non-uniform flow effect in the bundle described here is required only for the loop seal clearance phase.

The radial flow and enthalpy imbalance effects in the bundle on CHF are already accounted in the bundle factor in the 1986 AECL-UO CHF lookup table. [

]

[ ]

Reference:

1. Mitsubishi Heavy Industries, Ltd., Small Break LOCA Methodology for US-APWR, MUAP-07013-P (R0), July 2007.

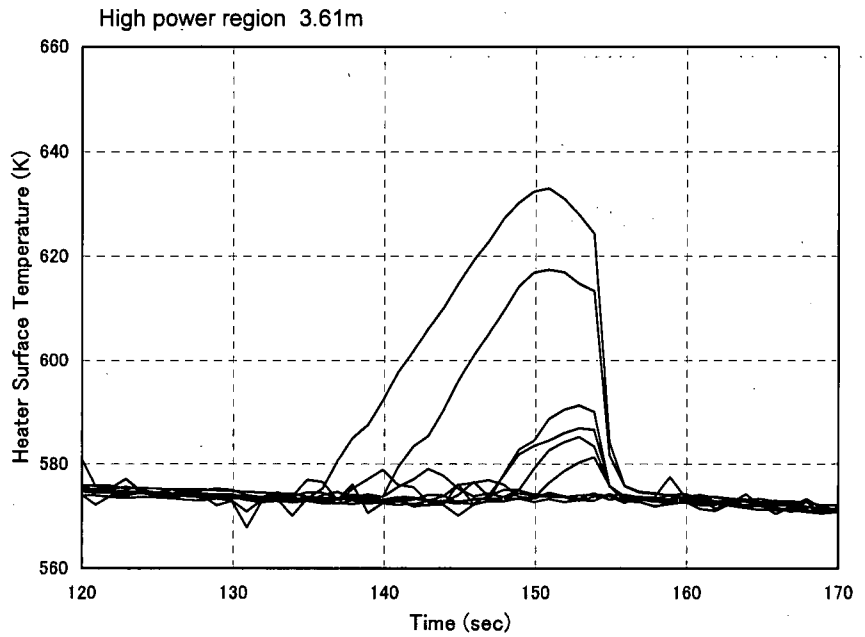

Figure RAI-8.2.1-19.1 Heater Rod Surface Temperature during Loop Seal Clearance Period at 3.61m

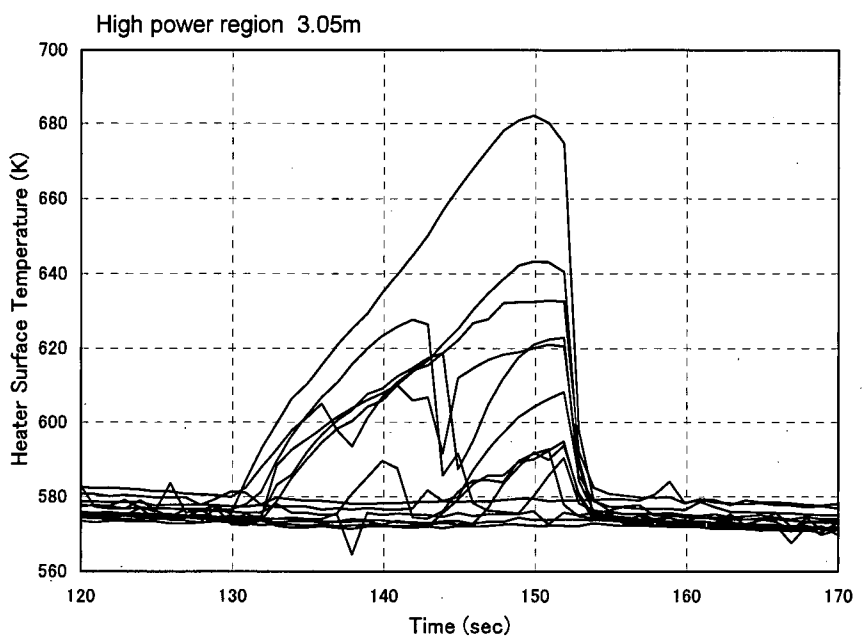

Figure RAI-8.2.1-19.2 Heater Rod Surface Temperature during Loop Seal Clearance Period at 3.05m

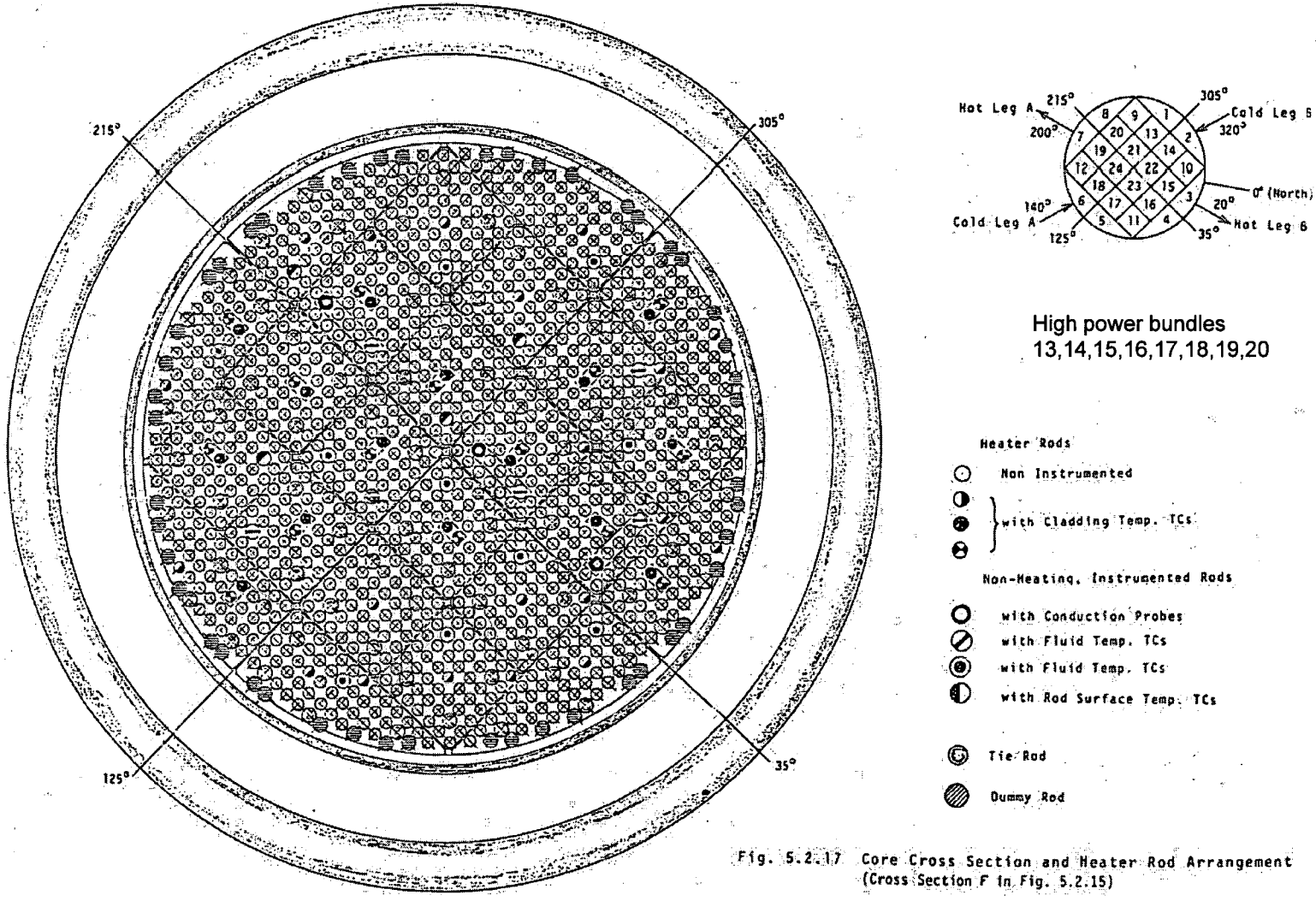

Figure RAI-8.2.1-19.3 Surface Temperature Measured Heater Rod location in the Bundle

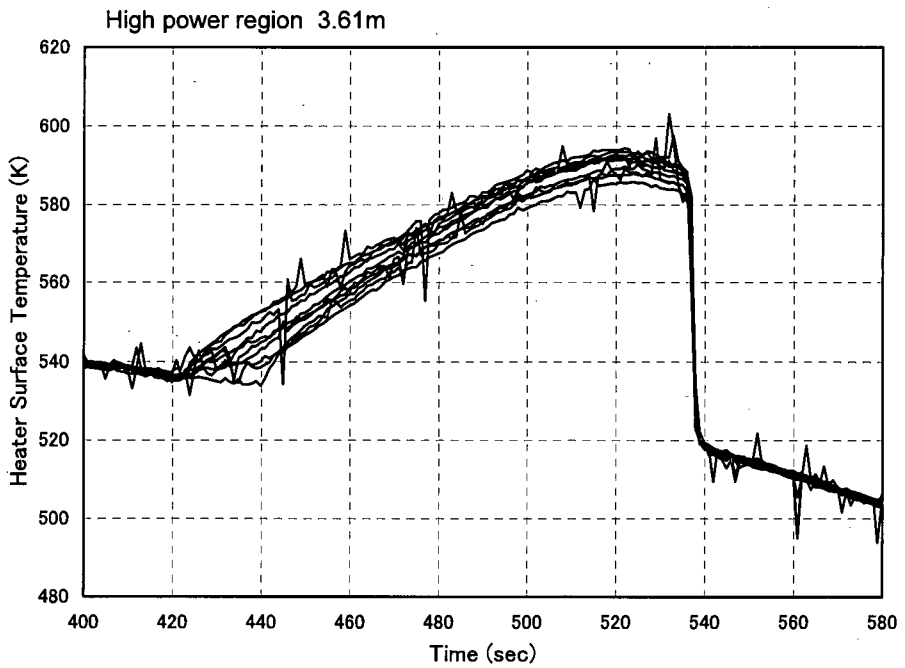

Figure RAI-8.2.1-19.4 Heater Rod Surface Temperature during Boil-off/Core-recovery Period at 3.61m

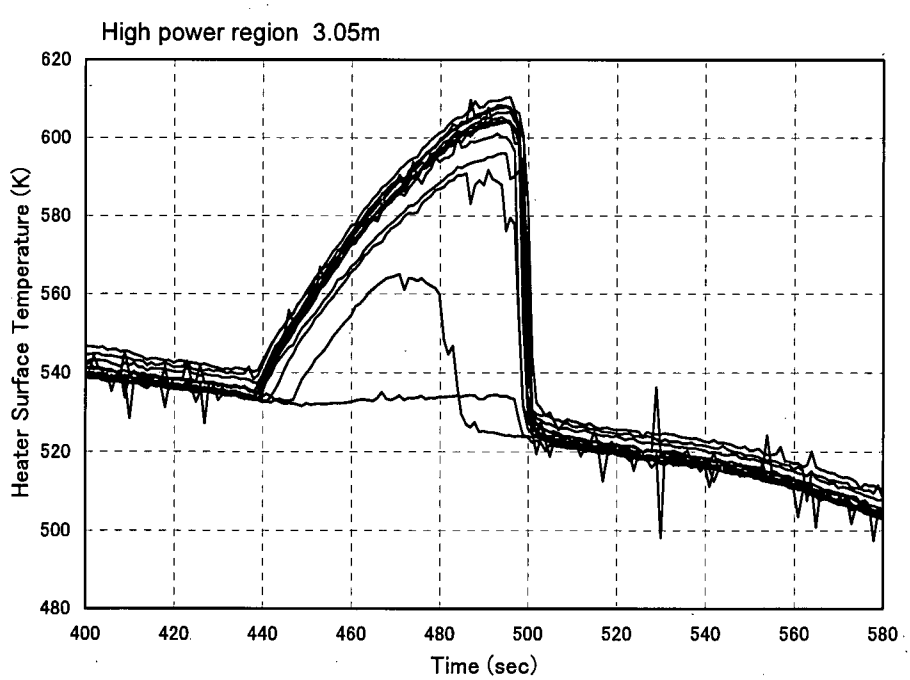

Figure RAI-8.2.1-19.5 Heater Rod Surface Temperature during Boil-off/Core-recovery Period at 3.05m

REQUEST CA-1

In Section 15.6.5 of the DCD, MHI identifies two small break LOCAs as being limiting for peak clad temperature: 1) a 7.5 inch break diameter SBLOCA (PCT = 774°F) which is the limiting case during the period of loop seal clearing and 2) a 1 ft^2 SBLOCA (13.5 inch break diameter) which is limiting during the boil-off phase (PCT = 1,317°F).

In comparison with other PWR designs that employ four coolant loops, the break size associated with SBLOCA most limiting case for the US-APWR (i.e., 13.5 in) is significantly larger. Typically the SBLOCA limiting break diameter for conventional Westinghouse-designed four-loop PWRs is on the order of 2 to 4 inches. The issue is the reason why the limiting break size is so much larger for the US-APWR.

Provide a discussion, substantiated by analysis, of the reasons why the US-APWR system design has such a different small-break LOCA response relative to conventional Westinghouse-designed four-loop PWR plants. Include a discussion of the design philosophy used in the US-APWR that may account for this difference.

RESPONSE

The following sensitivity calculations support to understand the characteristic of break spectrum for US-APWR SBLOCAs.

1) Enhanced Capacity of HHIS
   The flowrate capacity of the high-head injection system (HHIS) is greatly enhanced in the US-APWR to suppress the consequences of SBLOCAs, particularly for smaller break sizes. The injected flowrate of HHIS is a factor of [ ] times higher compared with that of the existent high-pressure injection system employed in typical 4-Loop PWRs. The HHIS provides the RCS with sufficient safety coolant to prevent the core from significant uncovery, resulting in lower PCT in comparison with the 4-Loop PWRs when smaller break sizes are assumed. In the case of larger break sizes, depressurization of the RCS becomes faster due to larger break flowrate, and thus the accumulator plays a primary role to suppress the fuel cladding heat-up.

   Table RAI-CA-1.1 compares calculated PCT results at the various break sizes when the HHIS capacity is reduced to [ ] of the nominal US-APWR specification with those results obtained for the US-APWR DCD Revision 2 (Ref. 1). This sensitivity study shows that the limiting PCT (1587 °F) appears at the 4-in break, which is smaller than the limiting break sizes for the US-APWR DCD calculations (7.5-in for the loop seal PCT 773 °F, and 1-ft^2 for the boil-off PCT 1323 °F). Transient evolutions under the 4-in break case are shown in Figures RAI-CA-1.1 through 13. The reduced HHIS is not able to provide the RCS with sufficient safety coolant to recover the coolant discharged out the break until the accumulator starts injecting the additional safety coolant at the low reactor pressure level. Consequently, the core uncovery continues for a long duration of the boil-off phase, resulting in higher PCT. This behavior is similar to that observed during a smaller break in the existent 4-Loop PWR.

2) Delay Time for Safety Coolant Injection
   One of the unique features in US-APWR is employing the gas turbine generator (GTG) for the emergency electric source instead of the existent diesel generator (DG).

The HHIS starts injecting safety coolant after generation of the ECCS actuation signal with a longer delay time of [ ], versus [ ] for the DG. A sensitivity result when the delay time is shortened [ ] is listed in the fourth line of Table RAI CA-1.1. This indicates that the PCT does not significantly increase by employing the GTG for US-APWR.

3) CCFL in Steam Generator
CCFL phenomenon at the SG inlet plenum and U-tubes plays an important role to form and clear the loop seal in the piping, which affects the PCT during loop seal period. As shown in Table RAI-CA-1.2, the SG primary-side flow area of US-APWR is remarkably larger than that of the existent 4-Loop PWR. The smaller flow area of the 4-loop PWR results in more severe liquid flooding (less liquid flow) compared to the US-APWR assuming that the same amount of steam flows into each SG and that the U-tubes have the same diameter.

[

]

The fifth line of Table RAI-CA-1.1 shows sensitivity results, where the analysis model is changed to cause more severe liquid flooding in the SG as mentioned above. Although the sensitivity calculation shows meaningful increase in PCT for the 7.5-in break case, no heat-up occurs for breaks smaller than 7.5-in. Therefore, the effect of CCFL in the SG does not significantly change the break size spectrum results in US-APWR SBLOCAs.

The US-APWR is designed such that consequence of SBLOCAs with smaller break sizes are sufficiently suppressed by its engineered safety features, particularly by the HHIS with the enhanced capacity. Although adoption of the GTG system for emergency electric sources requires a longer delay time to start the safety injection in the US-APWR, the PCT increase from cases with the shorter delay time is negligibly small in comparison with the PCT reduction accomplished by employing the HHIS. In addition, sensitivity calculations with the model that intentionally induces more severe flooding in the SG result in no significant heat-up during the SBLOCA with smaller break sizes less than

7.5-in.

To this end, the limiting PCT tends to occur in the SBLOCAs with larger break sizes in the break spectrum analysis for the US-APWR (Ref. 2).

References:

1. Mitsubishi Heavy Industries, Ltd., Design Control Document for the US-APWR, Chapter 15 Safety Analyses, MUAP-DC015, Revision 2, October 2009.
2. Mitsubishi Heavy Industries, Ltd., Small Break LOCA Sensitivity Analyses for US-APWR, MUAP-07025-P (R0), December 2007.

Table RAI-CA-1.1 Sensitivity Calculations Results (PCT)

Break Size	2-in	4-in	7.5-in
DCD Rev.2	No PCT*	No PCT	773°F (136s)**
SI Flow [ ]	No PCT	1587°F (1455s)	778°F (136s)
SI Delay (GTG -> DG)	-	-	733°F (130s)
CCFL (4-Loop PWR)	-	No PCT	843°F (144s)

*No PCT: Less than initial cladding temperature
**: PCT occurrence time

Table RAI CA-1.2 US-APWR Primary Reactor Design Specifications

Characteristics	PWR*	US-APWR	US-APWR/ PWR
Pressure (MPa)	15.5	15.5	1.00
Fluid temp. at hot leg (K)	598	601	1.01
Fluid temp. at cold leg (K)	562	564	1.00
Core			
Core power (MW)	3423	4540	1.33
Number of fuel rods	50952	67848	1.33
Number of unheated rods	4825	6425	1.33
Diameter of fuel rod (mm)	9.5	9.5	1.00
Diameter of unheated rod (mm)	12.2	9.7	0.80
Rod pitch (mm)	12.6	12.6	1.00
Hydraulic diameter of core (mm)	10.9		
Core height (m)	3.66		
Power density (MW/m^3)	9.9		
Core flow area (m^2)	4.75		
Core inlet flow rate (ton/s)	16.7		
Pressurizer			
Volume (m^3)	51		
Downcomer			
Downcomer flow area (m^2)	3.38		
Downcomer gap (m)	0.26		
Hot leg			
Diameter (m)	0.737		
Flow area (m^2)	0.427		
Cold leg			
Diameter (m)	0.699		
Flow area (m^2)	0.384		
Steam Generator (SG)			
Number of Tubes per one SG	3382		
Tube inner diameter (mm)	19.6		
Flow area per one SG (m^2)	1.02		
Length of SG tube (average) (m)	20.2		
Height from the top of heated part of core to the top of SG U-tube (m)	14.92		

* W-type 4-loop PWR in JAERI-M84-237 (ROSA-IV System description)

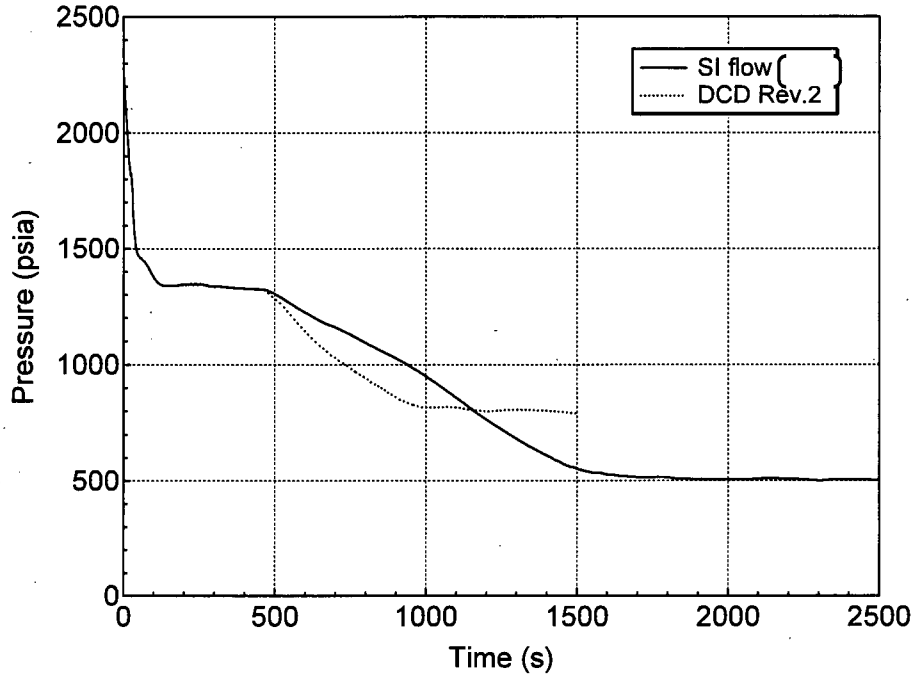

Figure RAI-CA-1.1 RCS Pressure Transient for 4-inch Break (Reduced HHIS Capacity)

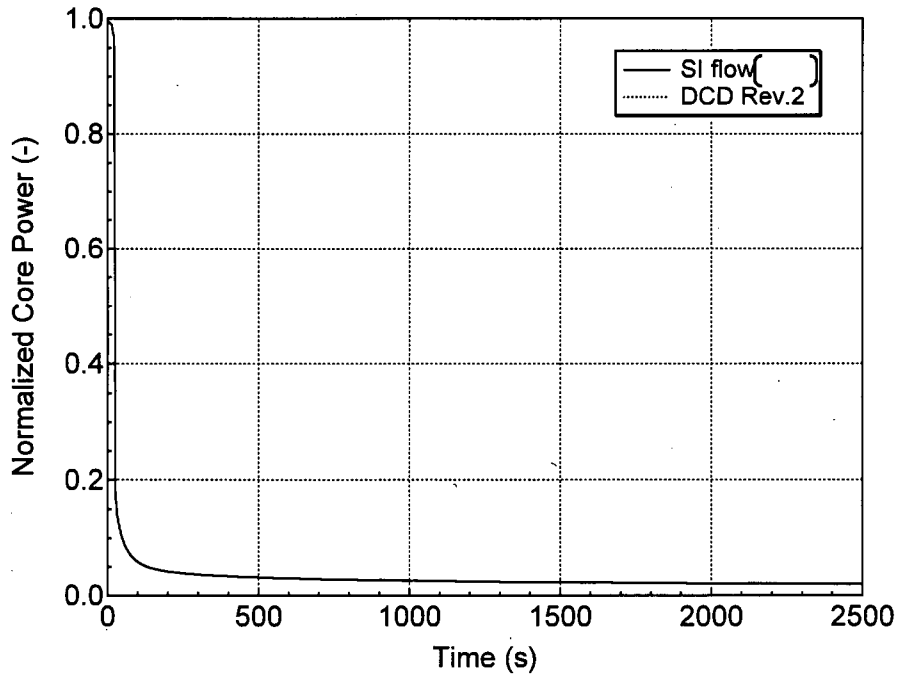

Figure RAI-CA-1.2 Normalized Core Power for 4-inch Break (Reduced HHIS Capacity)

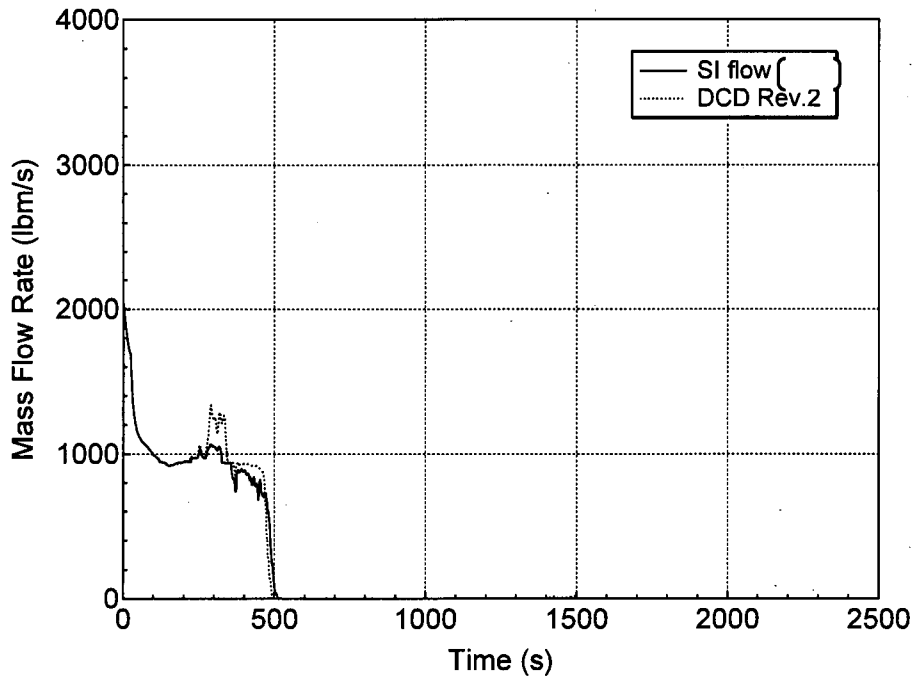

Figure RAI-CA-1.3 Liquid Discharge through the Break for 4-inch Break (Reduced HHIS Capacity)

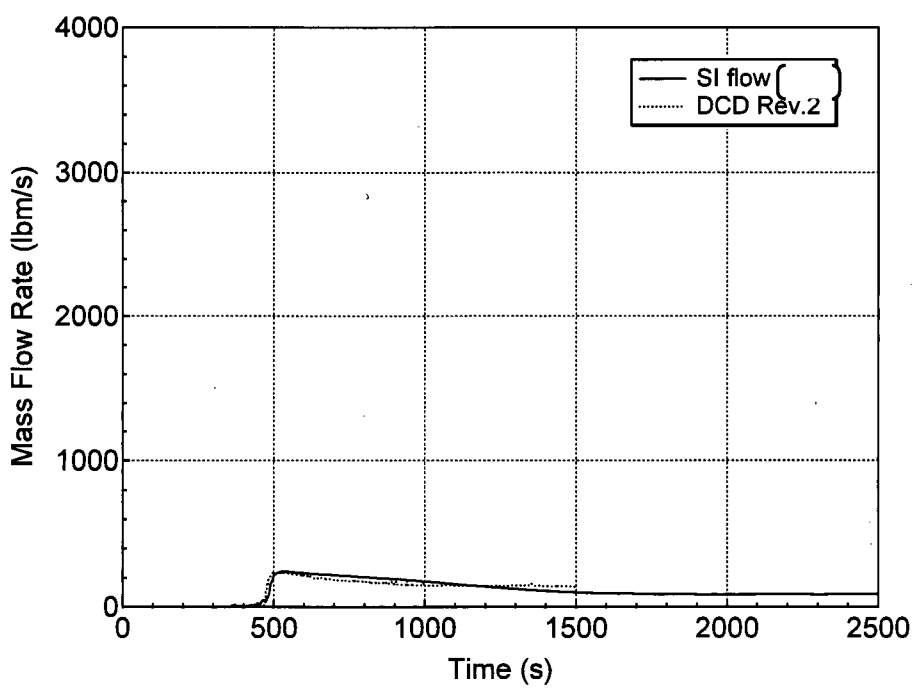

Figure RAI-CA-1.4 Vapor Discharge through the Break for 4-inch Break (Reduced HHIS Capacity)

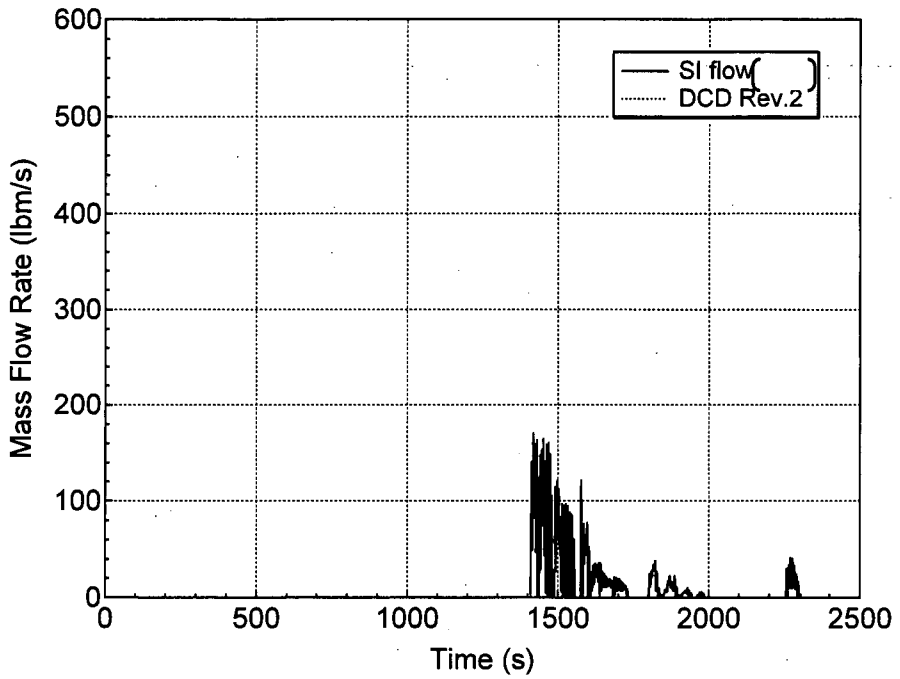

Figure RAI-CA-1.5 Accumulator Injection Mass Flowrate for 4-inch Break (Reduced HHIS Capacity)

Figure RAI-CA-1.6 Safety Injection Mass Flowrate for 4-inch Break (Reduced HHIS Capacity)

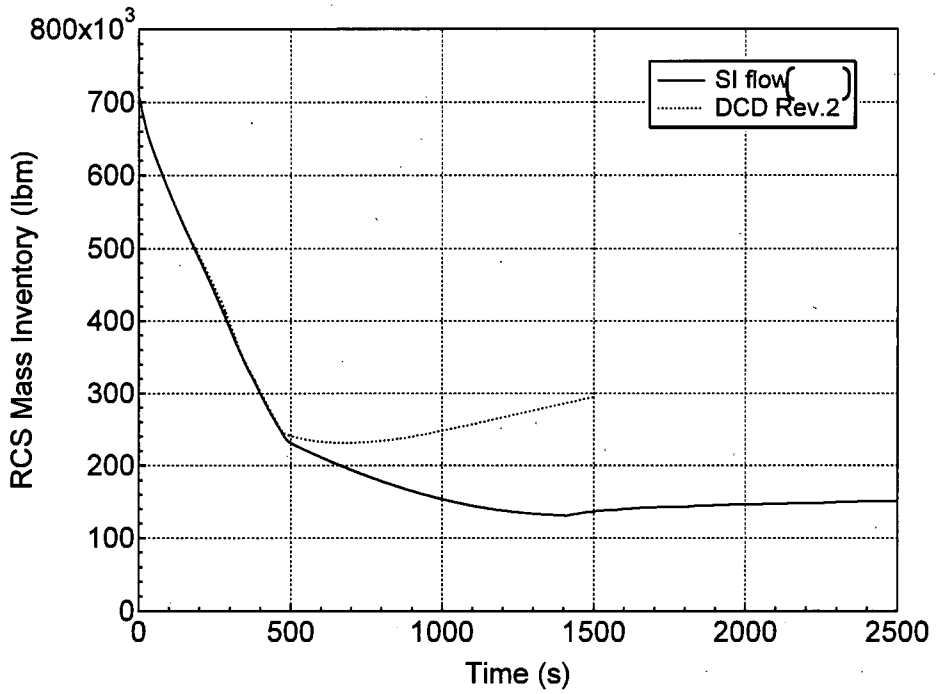

Figure RAI-CA-1.7 RCS Mass Inventory for 4-inch Break (Reduced HHIS Capacity)

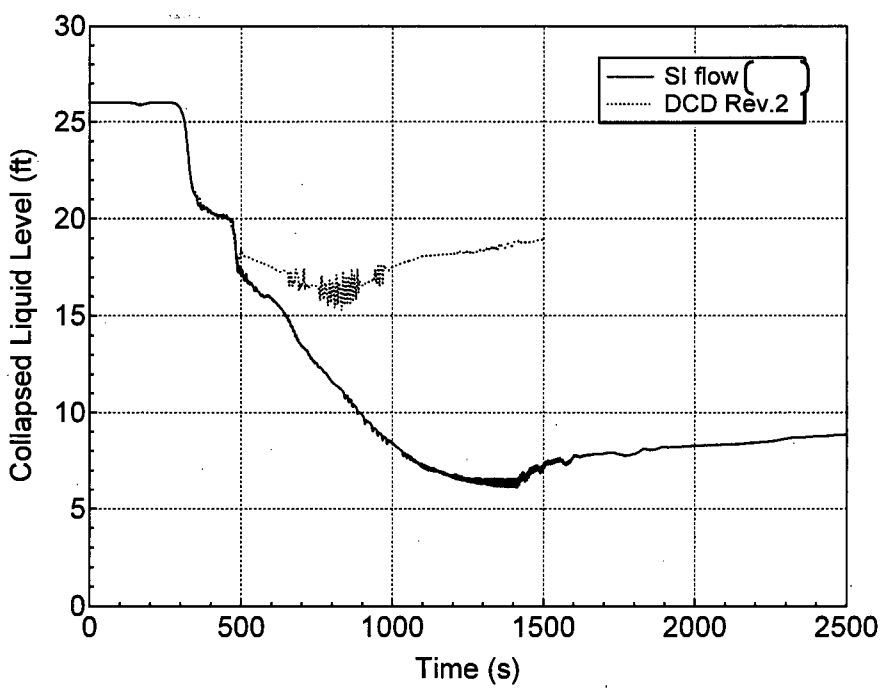

Figure RAI-CA-1.8 Downcomer Collapsed Level for 4-inch Break (Reduced HHIS Capacity)

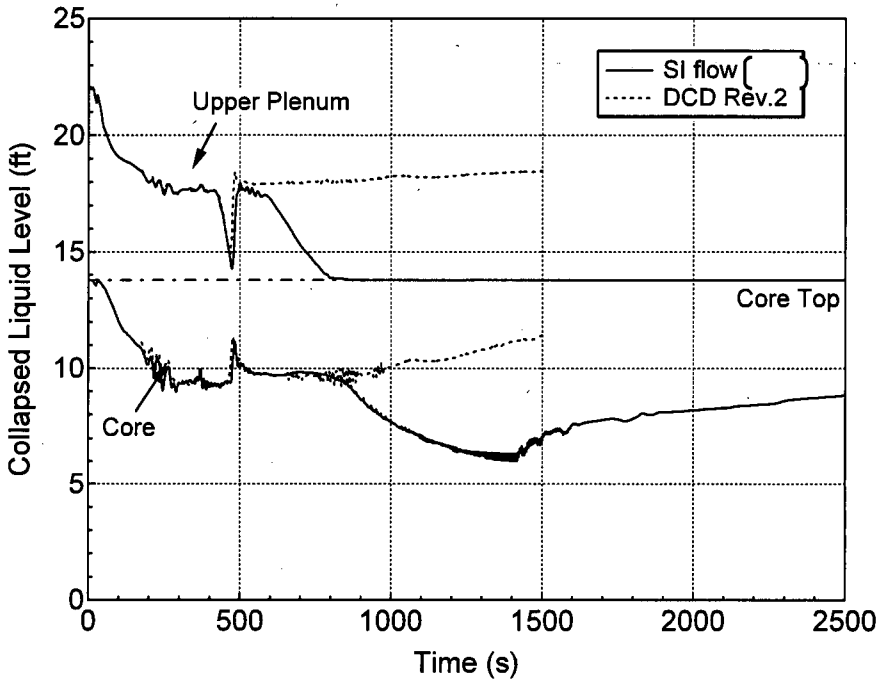

Figure RAI-CA-1.9 Average Core and Upper Plenum Collapsed Levels for 4-inch Break (Reduced HHIS Capacity)

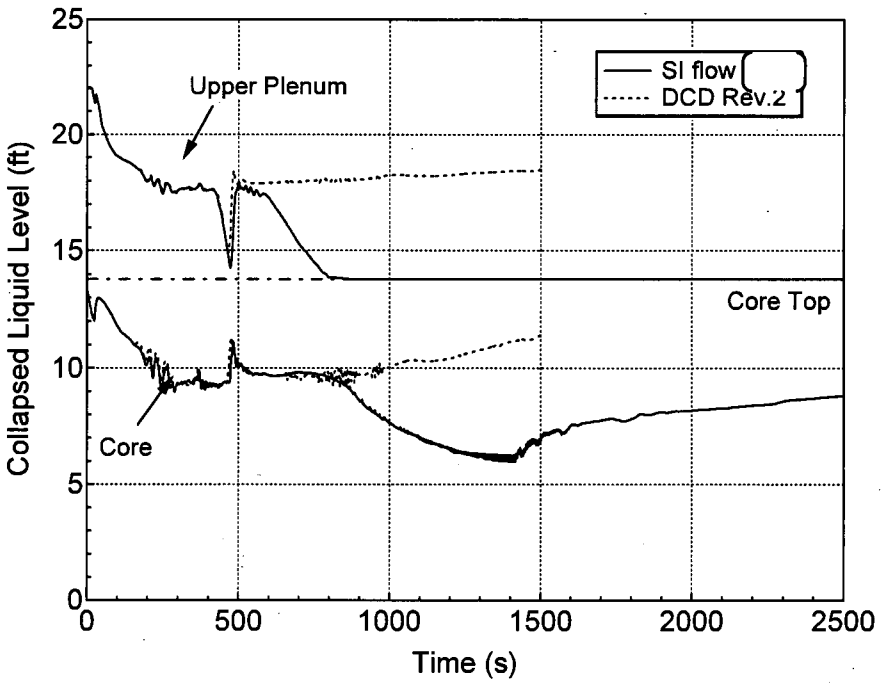

Figure RAI-CA-1.10 Hot Assembly and Upper Plenum Collapsed Levels for 4-inch Break (Reduced HHIS Capacity)

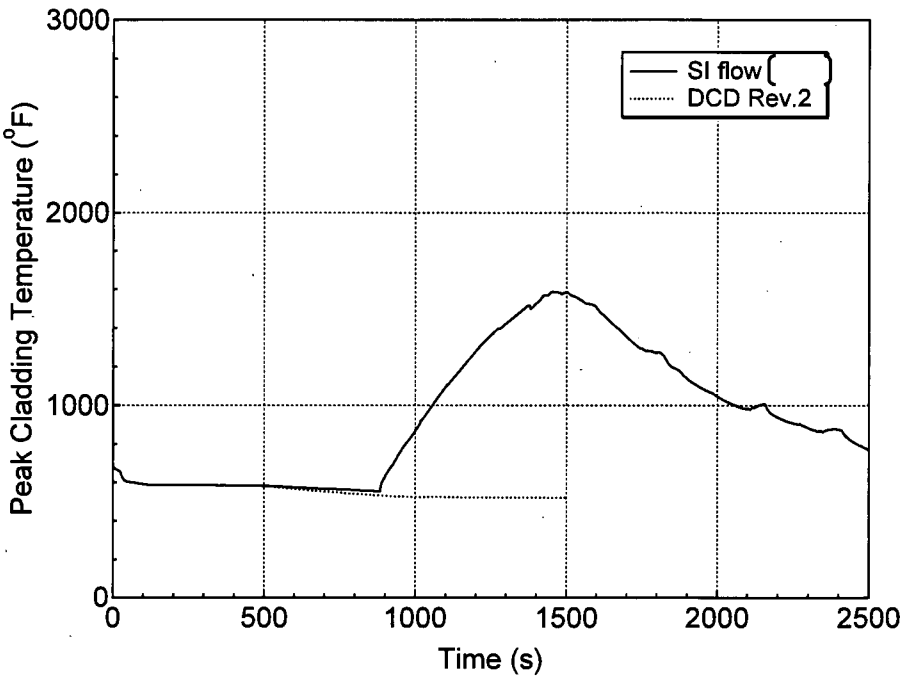

Figure RAI-CA-1.11 PCT at All Elevations for Hot Rod in Hot Assembly for 4-inch Break (Reduced HHIS Capacity)

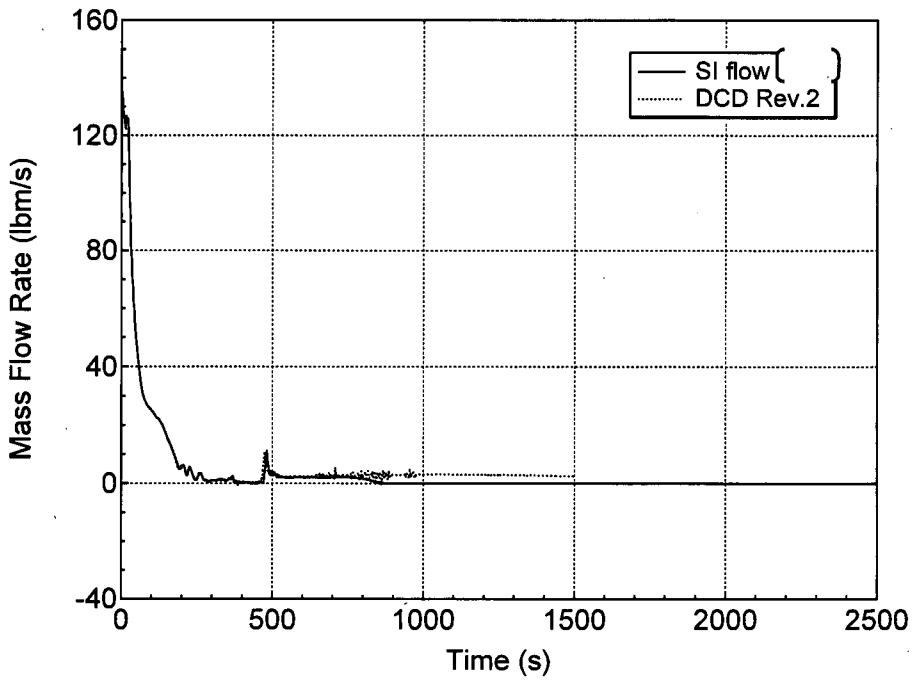

Figure RAI-CA-1.12 Hot Assembly Exit Liquid Mass Flowrate for 4-inch Break (Reduced HHIS Capacity)

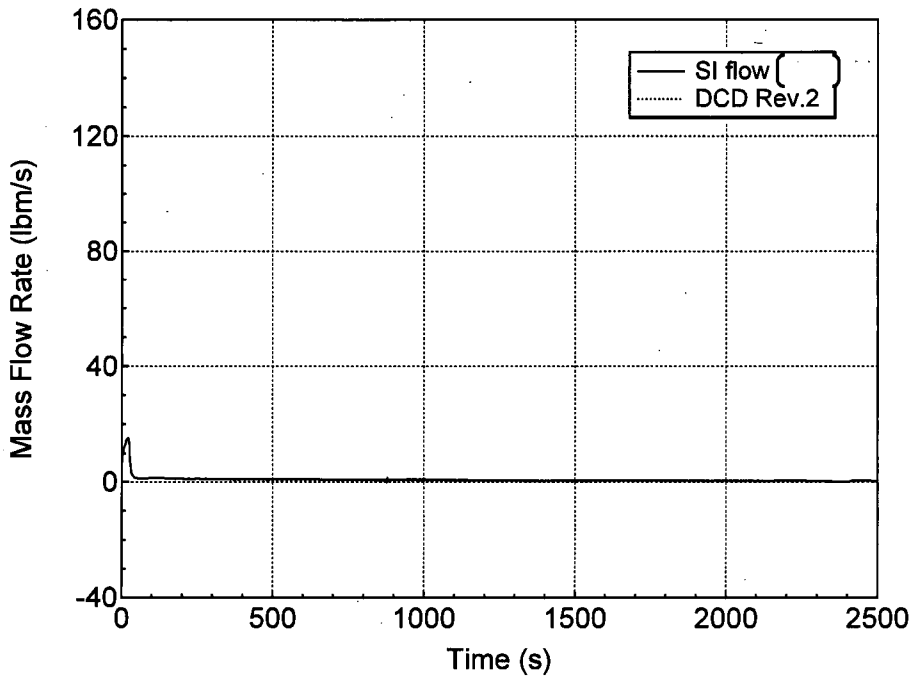

Figure RAI-CA-1.13 Hot Assembly Exit Vapor Mass Flowrate for 4-inch Break (Reduced HHIS Capacity)

REQUEST CA-5

[

]

RESPONSE

[

]

[

]

REQUEST CA-7

[

]

RESPONSE

[

]

[

]

[

]

[

]